The kinetics and mechanism of cure of an amino-glycidyl epoxy resin by a co-anhydride as studied by FT-Raman spectroscopy

J. Rocks[‡*], L. Rintoul[‡], F. Vohwinkel[†], G. George[‡1)]

[‡] Queensland University of Technology, Faculty of Science and CIDC, Brisbane 4001, Australia

[♣] ABB Corporate Research Ltd, Polymers & Electroceramics, 5400 Baden, Switzerland

[†]University of Applied Science, Laboratory of Organic Chemistry, 49009 Osnabrueck, Germany

[1)] to whom all correspondence should be addressed

Email: g.george@qut.edu.au (Graeme George)

Phone: +61 (0)7/386 422 03

Fax: +61(0)7/386 415 08

Abstract

The thermal curing behaviour of tetraglycidyl-4,4'-diaminodiphenylmethane (TGDDM) and a co-anhydride mixture consisting of maleic anhydride (MA) and hexahydrophthalic anhydride (HHPA) was studied from 55°C to 100°C by real-time FT-Raman spectroscopy. The quantitative changes in concentrations of anhydride, epoxy, and new-formed ester were measured and empirical reaction rate curves were constructed reflecting the kinetics of the curing process. After an induction period a simple kinetic scheme that is first order in both epoxy and anhydride monomer

consumption described the reaction profile until the reaction was influenced by chemo-rheological changes due to vitrification transition.

FT-Raman analysis revealed that curing propagation mainly occurs by polyesterification between epoxide and anhydride. Possible side reactions including the homopolymerization of MA are considered. The main side reaction is decarboxylation of MA that may produce some autocatalysis, but this is a minor contribution to the kinetics of cure. No conclusive evidence has been found for homopolymerization of MA or initiation of the curing reaction by the reaction product of TGDDM and MA, compared to the polyesterification.

Keywords: FT-Raman spectroscopy; epoxy-anhydride; cure kinetics

1. Introduction

Pierre Castan synthesized epoxy resins for the first time in the early 1940's. Many applications have been emerged and numerous epoxy monomers and hardener formulations have been developed since the first synthetic epoxy was produced. Nowadays, epoxy resins are intensively used in various technical applications such as coatings, composite matrices, potting compounds, or structural adhesives [1, 2].

To meet the relatively high thermal resistance criteria, especially for demanding aeronautical applications, aromatic amine-cured aminoglycidyl resins were developed [3]. Consequently, the curing behaviour and kinetics of such systems has been extensively studied by many different analytical methods such as DSC [4], gel permeation chromatography (GPC) [5], nuclear magnetic resonance (NMR) [6], and vibrational spectroscopy [7, 8] yielding a deep understanding of the reaction mechanisms involved. However, information on the curing behaviour of multifunctional aminoglycidyl resins in the presence of carboxylic acid anhydrides are rather limited, even when anhydride cured formulations show improved properties than amine cured

resins, *e.g.* less toxicity, higher glass transition temperatures, reduced water absorption, lower reaction exothermy and smaller shrinkage [1, 2, 9].

On the other hand the non-catalyzed anhydride-epoxy curing reaction is less reactive and hence demands a high reaction temperature ($\geq 120°C$) to initiate the curing reaction [10-12]. Using IR-analysis Steinmann [13] has proven that a non-catalyzed (acid or base) mixture of pure epoxy diglycidyl ether of bisphenol-A (DGEBA) with pure hexahydrophthalic anhydride (HHPA) does not react during a period of 24 hours at 100°C. This fact demonstrates the enormous disadvantage of anhydride-cured systems, which usually take long time intervals at high temperatures resulting in very expensive processing and handling steps.

Recently [14], an approach was shown that different non-catalyzed aminoglycidyl resins formulations have been cured with a co-anhydride mixture at relatively low curing temperatures, but still yielding high temperature properties (Tg > 200°C). However, all reported systems showed a major drawback – the presence of unreacted anhydride residues of the high melting pyromellitic dianhydride (PMDA) resulted in an inhomogeneous network structure [15]. To avoid the presence of partially undissolved hardener in these systems, we have cured a commercially available N,N,N',N'-tetraglycidyl-4,4'-diaminodiphenylmethane (TGDDM) with a low melting hardener mixture consisting of maleic anhydride (MA) and hexahydrophthalic anhydride (HHPA) [16]. This hardener combination not only results in a liquid eutectic mixture at room temperature but it can also be cured at ambient temperatures. However, the reaction mechanism has not been studied in detail.

The objective of this paper was to study the low temperature curing behaviour of the same epoxy/co-anhydride mixture by means of vibrational FT-Raman spectroscopy under isothermal conditions. As a complementary technique to mid infrared spectroscopy, FT-Raman is able to provide fundamental vibrational information. Based on the different selection rules of these two spectroscopic techniques, polar bonds tend to yield strong IR and weak Raman bands, whereas non-polar groups give rise to strong

Raman and weak IR bands. FT-Raman also allows one to monitor the curing reaction over the complete conversion range, although the material undergoes several state transitions during curing, i.e. gelation and vitrification. These transitions have only a limited influence on the vibrational spectrum. The quantitative aspects of FT-Raman spectroscopy permit quasi real time *in situ* studies of the crosslinking reaction and the direct calculation of the concentration profiles of various reactive species. Further advantages compared to mid-IR are the lack of interferences from water vapor and glass, which is very convenient because glass sample containers can be used during experiments. Kinetic analysis from the conversion of the functional groups and the obtained empirical rate curves are discussed in the light of proposed reaction mechanisms for the uncommon cure behaviour of the uncatalyzed TGDDM/MA/HHPA-system.

2. Experimental

2.1. Materials

The epoxy resin used was a commercial Araldite®MY721, mainly based on N,N,N',N'-tetraglycidyl-4,4'-diaminodiphenylmethane (TGDDM), supplied by Vantico, Switzerland. A combination of two hardeners was used, maleic anhydride (MA) and hexahydrophthalic anhydride (HHPA), to cure the TGDDM monomer. Both anhydrides were supplied by Fluka, and utilized without further purification. The chemical structure of the used materials is shown in Fig. 1. The mixing ratio was 100/48/32 (TGDDM/MA/HHPA) by weight, reflecting a stoichiometric anhydride to epoxy ratio, r, of 0.8.

The epoxy monomer was preheated to 65°C to reduce the viscosity of the MY721-resin, before the premixed hardener-mixture was added and dissolved with an Ultraturrax-high shear mixer at 13.500 rpm for 5 minutes to obtain a homogeneous mixture. To prevent a temperature rise and any further reaction during mixing, all samples were cooled during

the mixing process in ice water. Afterwards, the mixture was degassed for 3 minutes at pressures below 10 mbar and stored in liquid nitrogen to prevent further curing.

2.2. FT-Raman Spectroscopy

All spectroscopic experiments were carried out on a Perkin-Elmer System 2000 NIR FT-Raman spectrometer, equipped with a diode pumped Nd-YAG laser (λ=1064nm) as an excitation source and a room temperature InGaAs photoelectric detector. The backscattered radiation was collected at 180° to the excitation. Typical spectra were recorded in a range of 200 to 3800 cm^{-1} at a laser power of 320 mW. Every 4 minutes a spectrum was collected consisting of 32 co-added scans with spectral resolution of 8 cm^{-1}. The premixed epoxy mixture (4$\pm$0.2 g) was filled in a NMR sample tube and placed in the preheated heating block under isothermal conditions at 55, 65, 75, and 100°C, respectively. The steady state temperature was controlled with an accuracy of ±0.2°C. Spectra were recorded from the moment the tube was introduced in the heating block. To reach the ultimate conversion some samples were also post-cured at 150°C for 1 hour.

2.3. Gas Chromatography

A two column micro gas chromatograph (MTI M200H) equipped with a 8m Poraplot Q and a 10m molecular sieve (5 Å) column was used to separate the trapped gaseous byproducts during an isothermal curing reaction at 65°C. Helium was used as a carrier gas with a flow rate of 10 ml/min. Continuous data acquisition was carried out every 3 minutes until the samples reached the point of gelation.

3. Results and Discussion

3.1. Thermal Cure Reactions

The epoxy group is characterized by its reactivity towards nucleophilic and electrophilic species and thus it is reactive to a wide range of reagents. The formation of polyester for the non-catalyzed reaction of epoxy monomers and cyclic carboxylic acid anhydrides has been intensively studies during the last years. The generally accepted stepwise reaction mechanism is schematically shown in Fig. 2(a) [17-22]. In the early stage of cure, the reaction mechanism involves the presence of hydroxyl groups, which act as an initiator for the reaction. The hydroxyl groups are present as a substituent on a fraction of the epoxy molecules that have oligomerised on synthesis. An attack of hydroxyl groups on the anhydride molecules results in a monoester having a free carboxyl group (reaction 1). This free carboxyl group (monoester) then reacts with the epoxide to yield a diester and a new secondary hydroxyl group (reaction 2) thus perpetuating cure (reaction 3). The evidence that the quantities of mono– and diester produced are equal to the amount of consumed anhydride confirmed these reactions. It has also been reported that, at least up to vitrification, there is no significant difference in the consumption of epoxy and anhydride groups [23]. The observation that the number of epoxy groups at higher conversions decreases faster than the increase in the diester groups can be attributed to the etherification reaction. This reaction occurs between the epoxy and hydroxyl groups under the catalytic influence of anhydride or carboxyl groups (reaction 4), which constitutes a significant side reaction. However, the direct polyetherification is considered of little significance here, since the curing temperatures are below 180°C for TGDDM system [8].

An essentially different mechanism occurs when strong Lewis bases, e.g. tertiary amine, imidazoles or ammonium salts, are used to catalyze the polymerization. In case of technical monomers, the curing reaction might be described as shown in Figure 2(b), although the reaction mechanism has been subject of considerable controversy in the past [13, 38-46]. It is proposed that the tertiary amine reacts with the epoxy monomer and forms a zwitterion that contains a quaternary nitrogen atom and an alkoxide as

shown in Figure 2(b), reaction (5). The alkoxide rapidly reacts further with an anhydride group leading to a carboxylate anion as shown by reaction (6). This carboxylate anion may be considered as active center for the chainwise alternating co-polymerization. Propagation occurs through the reaction of the generated carboxylate with an epoxy group and the accompanied formation of new alkoxide anion, reaction (7),

This, in turn, reacts at a very fast rate with an anhydride group regenerating the carboxylate anion, cf. Figure 2(b), reaction (8).

There is still no definite validation regarding the termination step and whether the initiator remains chemically attached during the whole course of the reaction. Some authors describe an irreversible bonding of the initiator [43] but there is disagreement on this point [13, 44].

3.2. Functional group analysis

The spectra of the unreacted MY721 epoxy monomer as well as the two carboxylic acid anhydrides can be seen in Fig. 3. Detailed peak assignments of the main absorption bands are listed in Table 1. The band assignments were made according to standard spectroscopy literature [24-26] and by considering results of previous Raman studies [27, 28]. In the spectrum of MY721 three of the bands attributable to the epoxy ring are easily observed. These are located at 3072 cm^{-1} [ν_{as} (CH$_2$) and 3001 cm^{-1} [ν_s(CH$_2$)] due to C-H groups of the epoxy ring and at 1260cm^{-1} [breathing of the epoxide ring]. The bands at 907 cm^{-1} [ν_{as} ,epoxide ring deformation], and 866 cm^{-1} [ν_s ,epoxide ring deformation] are much weaker and overlap with anhydride bands. In the spectra of the crystalline anhydrides the bands of major interest are those due to the vibrations of cyclic anhydride groups, such as the intense symmetric and antisymmetric stretch of the carbonyls at 1840 and 1780cm^{-1}, respectively. This is because the anhydride group is the reactive center and the bands would be expected to decrease during curing with the epoxy.

FT-Raman spectroscopy was performed during real-time monitoring of the curing process. It was assumed, and later confirmed by the experiments, that the aromatic hydrocarbon groups, corresponding to the characteristic vibration at 1615cm^{-1} [aromatic quadrant stretch], are not involved in the curing reaction and hence the peak area does not change over the entire curing period. Therefore, the invariant peak at 1615 cm^{-1} was used for all spectra as an internal normalization standard [27, 28].

From the recorded intensity data, the fractional consumption of functional groups, α, can be calculated by equation 1:

$$\alpha(t) = 1 - \left(\frac{I_{(t)}}{I^{1615}} / \frac{I_{(0)}}{I^{1615}} \right)$$

eq. 1

where I_o, I_t, are the relative intensities of reactive species at time zero, and after a certain time interval, t, of the cure cycle. Due to the epoxy excess ($r<1$), the concentration curves of epoxy and anhydride groups can be directly compared only if we consider the absolute conversion. In terms of spectroscopic parameters, the absolute conversion is given by $C_0\alpha(t)$, where C_0 refers to the initial concentration of the reactive species.

Curing data obtained after different reaction times and reaction temperatures are shown for the MY721/MA/HHPA-system with a molar anhydride to epoxy ratio, r=0.8, at 65°C in Fig. 4 and Fig. 5. Interferences from thermal emission bands or fluorescence, as reported by Walton and Williams [28], were not obtained. Subsequently, the spectral changes were monitored quantitatively and detailed results are discussed in the following paragraphs.

Anhydrides:

The peaks from the mixture at 3111, 1850, 1780, 1060, 868, and 636cm^{-1}, respectively, can be assigned to the two anhydrides. Peaks corresponding to the individual MA and HHPA components are not reliable due to peak overlap with the epoxy monomer. Hence, although a clear band due to MA is seen at 3111 cm^{-1}, in the

presence of the epoxy, the respective functional groups consumption of the two anhydrides, hexahydrophthalic anhydride and maleic anhydride, cannot be further differentiated by FT-Raman spectroscopy. However, it can be expected that both anhydrides compete for the reaction with epoxy groups as shown in Fig. 6, even when the two anhydrides show similar overall reactivity as reported in [16] for the same system.

All anhydride functional group peak intensities decrease progressively throughout the entire cure. The total conversion of the functional anhydride groups can be gained using the typical anhydride ring vibrations at 1850 and 1780cm^{-1} [ν_s (C=O) and ν_{as} (C=O)], and 1060cm^{-1} [ν_{as} (C-O-C)], respectively. In this study the reaction of anhydrides was followed by means of the 1850cm^{-1} [ν_s (C=O) of the anhydride ring] as proposed in the past [29] and the results are illustrated in Fig. 6(a). To convert peak areas for the evolution of anhydride concentration, *[Anh]*, as shown in Fig. 6(b), the initial anhydride concentration of 3.89 mol/kg was considered. It can be seen that the anhydride peaks have not fully extinguished at lower curing temperatures and hence the anhydride concentration curve stabilized on a quasi-stationary plateau after a certain time period. This observation can be explained by the fact that the anhydride consumption is limited due to a physical liquid-to-solid transformation of the material. From this point, the reaction becomes diffusion controlled and a significant decrease of the reaction rate is observed; see Fig. 6(b). To reach a complete conversion of the reactive groups isothermal curing temperature above 75°C or extended post curing steps are necessary.

Epoxide:

A typical decrease of peak intensities corresponding to the epoxy group consumption at 3072, 3008 and 1260 cm^{-1} can be observed during the entire curing reaction. The epoxide ring breathing vibration at 1260cm^{-1} is well-resolved and essentially Lorentzian shape, as seen in Fig. 7(a). Hence this was utilized to monitor the epoxy conversion as

proposed previously [27, 30]. To enable peak height measurements a baseline

correction was performed and an initial epoxide concentration of 4.72 mol/kg was

considered to create the epoxide group concentration profile. A plot of the epoxide group

concentration, *[EP]*, over time for different temperatures is given in Fig. 7(b). A sigmoidal

curve with a slower initial rate of consumption followed by a steady rate before a

decrease at longer time, is obtained for all curing temperatures. This is more obvious at

the lower cure temperatures (1) and (2) in Figure 7(b). It can be seen that at curing

temperatures below 100°C the crosslinking reaction is quenched by a liquid to solid

transition before it can reach the 100% conversion. This behaviour is consistent with the

observed anhydride consumption behaviour. At an isothermal curing temperature of

55°C almost 68% of epoxy groups were converted, while during a curing at 75°C, 76% of

epoxide groups were converted. However, it can be expected that the polyesterification

reaction will continue also into the glassy state, but at a significantly decreased reaction

rate.

Ester groups:

The relative increase of bands due to ester group formation upon cure can be

observed at 2963cm^{-1} [ν_{as} (CH$_2$) adjacent to the ester group], and 1734 cm^{-1} [ν (C=O)

aliphatic ester]. The latter total aliphatic ester peak contains both monoester and diester

contributions and was used to determine the extent of curing reaction according to eq. 2

as:

$$\beta = \frac{\left(\dfrac{I^{1730}_{(t)}}{I^{1615}} - \dfrac{I^{1730}_{(0)}}{I^{1615}}\right)}{\left(\dfrac{I^{1730}_{(\infty)}}{I^{1615}} - \dfrac{I^{1730}_{(0)}}{I^{1615}}\right)} \qquad\qquad \text{eq. 2}$$

where β is the extent of the esterification reaction, I_t, the Raman intensity at time, t,

and I_0 corresponds to the intensity at $t=0$, and I_∞ is the intensity at time of curing

completion, $t=\infty$. It was assumed that the ultimate conversion ($t=\infty$) of reactive groups was reached after a postcuring-step at 150°C for 1 hour.

The total formation of aliphatic ester groups during the curing reaction at different temperatures is given in Fig. 8. An extended delay before start of the ester formation as reported by Stevens [21, 22] was not observed. Besides, it can be seen that ester formation approaches a limiting value at long curing times, which is an agreement with the anhydride and epoxy consumption behaviour.

Side reactions:

The disappearance of the characteristic C=C vibrations from maleic anhydride at 3111cm^{-1} [ν (=C-H)], 1590cm^{-1}[ν (C=C)], and 636cm^{-1} [γ (=CH-H)] is clearly visible in Fig. 5. Detail of the region from 1670 cm^{-1} to 1570 cm^{-1} is shown in Fig. 9(a) and the decrease in the C=C band intensity of MA at 1590 cm^{-1} and an increase in a broad band that first appears as a shoulder around 1640 cm^{-1} are shown in Fig. 9(b) and 9(c) respectively. This could suggest that the unsaturation of maleic anhydride is being consumed at low temperatures. If so, then it could provide evidence for the reaction of maleic anhydride by anionic initiated homopolymerization through charge-transfer reactive intermediates zwitterions as reported by Zweifel *et al.* [31] and Ricca *et al.* [32] and depicted in Fig. 10 (step 1). Maleic anhydride is difficult to homo-polymerize by a conventional free radical or anionic initiator, but it can be initiated by nitrogen bases to yield poly(maleic anhydride). The monomer is an excellent organic electron acceptor and hence it forms zwitterions with a suitable base. In the investigated system the zwitterions could, in principle, be directly formed in the presence of nitrogen bases (TGDDM monomer) at room temperature and appear to be the true initiator for poly(maleic anhydride) as shown in Fig. 10 (step 2). An indication for the zwitterions formation is given by the immediate color change of the mixture, from light yellow to dark red, as soon as maleic anhydride was added. This amine activated color change of maleic anhydride has been observed earlier for maleic functional copolymers [33, 34] and was

related to the formation of zwitterion intermediates. However, a more detailed analysis of this spectral region suggests that the changes may be linked to the primary esterification reaction and result from changes to conjugation following ring opening of MA. The evidence for this may be seen from an analysis of the extended spectral region shown in Fig. 11(a). This is evidenced by the isosbestic point in the spectrum at 1760 cm^{-1} that supports the smooth conversion of anhydride (1780 cm^{-1}) to ester (1734cm^{-1}) that parallels the changes in the MA band at 1590 cm^{-1} and the growth of the broad band near 1640 cm^{-1}. This is shown in Fig. 11(b) in which the intensities of the four bands are plotted during cure. They appear to all follow the same kinetic relationship so that the change in the band at 1590 cm^{-1} is most probably a result of the ring opening reaction of the MA producing a change in the conjugation of the C=C rather than its actual consumption. The broadening of the band at around 1640 cm^{-1} most probably reflects the range of environments that the C=C encounters after ring opening as cure takes place.

Evidence for a chemical side reaction, the spontaneous decarboxylation of MA accompanied by water release, is given by carbon dioxide and water formation as determined by *in situ* gas chromatography, see Fig. 12. This observation is in agreement with previous studies [32, 35], although the exact mechanism remains unclear. The observed CO_2 generation can be related to the decarboxylation of maleic anhydride initiated by the presence of the tertiary amine structure of MY721, since no CO_2 was detectable when utilizing HHPA as sole curing agent.

The absence of a broad band at 1080cm^{-1} [ν (C-O)] shows that no ether groups were formed, even at curing temperatures up to 150°C, supporting the statement that polyetherification, as illustrated in Fig. 2 (step 4), is effectively suppressed. This is in accordance with earlier results obtained by Tanaka and Kakiuchi [23], Fischer [36], and Luston *et al.* [37]. Additionally, we were unable to observe changes of the peak position and intensity at 1615cm^{-1} [aromatic quadrant stretch] of FT-Raman spectra that supports

the hypothesis that a "back-biting" cyclization of chlorohydrin impurities in MY721 at higher curing temperatures as reported by St. John *et al.* [27, 31] does not occur.

3.3. Rate curves and kinetic analysis

Empirical rate curves were generated for the different reaction species by applying a weighted smoothing function using a minimum number of iterations to obtain a curve. This procedure ensured that the instantaneous reaction rates obtained from the concentration profiles were not affected by single data point scattering.

To study this epoxy/anhydride reaction the empirical rate curves were calculated by taking the first derivative of the epoxy concentration versus time data (Fig. 6) as shown in Fig. 13(a). The obtained rate curves have a pronounced maximum which, in the reaction scheme, may represent the development of the steady state concentration of the reactive intermediates. This behaviour is more pronounced at lower isothermal curing temperatures. Assuming a non-catalyzed mechanism this induction period is reflecting the generation of intermediate COOH and OH-groups. While, considering a catalyzed reaction mechanism the presence of an induction period can be attributed to a rather slow initiation step when polymerizing at low temperatures.

An alternative explanation for the maximum in the rate curve, Fig. 13 (a), is that it indicates the reaction is autocatalytic in nature. Autocatalysis is observed when the tertiary amine structure of the TGDDM-monomer acts as catalyst in epoxy /anhydride curing reaction. A further possible source of any autocatalytic contribution could be reaction products between MA and the aminoglycidyl monomer, as discussed before, and schematically shown in Fig. 10. These reaction products, especially the proposed formation of carboxylate anions, could act as an additional initiator in the curing reaction. Despite, the catalyzed reaction mechanism has obviously an autocatalytic nature; isothermal kinetic runs have been analyzed with an excellent agreement by first-order kinetics, particularly under isothermal curing conditions [42]. To account for this

observation, Riccardi and co-workers [45] developed and experimentally validated a mechanistic model that predicts a chainwise polymerization proceeding by an anionic mechanism (epoxy/anhydride/tertiary amine) an induction period followed by first-order kinetics when using low isothermal cure conditions. Therefore, it was considered here that it is not necessary to invoke autocatalysis in order to explain the observed concentration profiles obtained from spectral data.

The measured data for the consumption of the epoxy groups are shown in a linearized first-order kinetic plot in Fig. 13(b). It can be seen that the reaction obeys first order behaviour $[(1-\alpha)^1)]$. For an extent of conversion of around 70%, a significant drop in the experimental reaction rate is observed due to diffusional restrictions indicating the change of the reaction mechanism from kinetic to diffusional control. Therefore, the apparent first-order rate constants were calculated as a function of temperature from the initial slopes and are listed in Table 2.

Assuming the Arrhenius dependency of the rate constant on temperature, as depicted in Fig. 13 (c), an activation energy of 71.01kJ/mol and a frequency factor of 19.85 min^{-1} was calculated, respectively. This obtained activation energy is in excellent agreement with other studies where the activation energy for base catalyzed anhydride/epoxy curing reactions is reported in the range of 70-75 kJ/mole [42, 46].

3.4. Cure mechanisms

The overall curing pattern clearly indicates that the network mainly consists of ester linkages built by polyesterification. The observed reaction rates for the studied curing temperatures are significantly higher than values reported for the non-catalyzed curing reaction [13]. This observation provides an indication that the thermal cure of the investigated TGDDM/MA/HHPA-system is probably catalyzed by the tertiary amine structure of the TGDDM-monomer used. Hence, the curing reaction favors an anionic alternating chain-polymerization as shown in Figure 2(b). However, the experimentally obtained FT-Raman data cannot be unambiguously used to clearly differentiate between

a non-catalyzed and a catalyzed mechanism, because the expected new vibrational bands are overlapped with conjugated species from the MA (cf. 3.2). By plotting the empirical data in an epoxy-anhydride conversion-conversion diagram, it is possible to establish the stoichiometry of the reaction and to detect possible changes of the mechanism with conversion. A plot of this type is shown in Fig. 14 for the investigated system cured at 65°C. It can be seen that all data points can be exactly accommodated on a single master curve. In particular, over the complete isothermal low temperature curing, the data fit to an iso-conversion line with a slope equal to one. This indicates a mechanism whereby, in the presence of sufficient concentration of hardener, a single epoxy group reacts with one anhydride group in an alternating co-polyesterification. However, from the data presented here it is not possible to distinguish between the two anhydrides, hence it is not known if both anhydrides were consumed at an equal rate. Moreover, the good fit to the iso-conversion line indicates that the dominance of polyesterification excludes the potential polyetherification side reaction, e.g. homopolymerization, in the investigated temperature range. However, the curing proceeds not only by the polyesterification reaction between anhydride and epoxy. Especially at higher curing temperatures a significant amount of TGDDM (tertiary amine) initiated homopolymerization of maleic anhydride has been identified.

4. Conclusions

FT-Raman spectroscopy has been used to monitor the anhydride/epoxy curing reaction. Fluorescence and thermal emission does not cause a problem in the spectra and satisfactory signal to noise ratios were obtained. Quantitative concentrations of epoxy, anhydride and ester groups have been measured during the cure of TGDDM/MA/HHPA at temperatures between 55°C to 120°C using FT-Raman spectra. Conversion data of the functional groups were determined and used to evaluate the reaction mechanisms. It was shown that the investigated anhydride-cured epoxy system reacts mainly by polyesterification . Calculated rate curves clearly indicate a first-order curing reaction. Analysis of the FT-Raman spectra showed that the total anhydride and epoxy consumption, as well as the ester formation follows first order kinetics up to the point where the reaction becomes diffusion controlled ($\alpha \sim 70\%$) with an Arrhenius dependency of the rate coefficient on temperature. The calculated reaction rates for the anhydride and epoxy monomer consumption provides some indication that the curing reaction is probably base catalyzed by the tertiary amine structure of the TGDDM-molecule.

Evidence has been found by gas chromatography for decarboxylation and the release of water. The formation of these reaction products could contribute to an autocatalytic curing reaction but the kinetic analysis does not indicate autocatalysis is significant under the conditions of low-temperature cure.

5. Acknowledgement

6. References

[1]   Ellis B., Chemistry and Technology of Epoxy Resins, 1, Glasgow, Blakie Academic Professional, 1993.
[2]   May CA., Epoxy Resins, New York, Marcel Dekker, 1988.
[3]   Lin SC, Pearce EM., High-Performance Thermosets - Chemistry, Properties and Applications, Munich, Carl Hanser Publisher, 1994.
[4]   Barton JM. Adv. Poly. Sci. 1985; 72:111.
[5]   Rogers RN, Smith LC. Analytical Chemistry 1967; 39:1024.
[6]   Grenier-Loustalot M, Grenier P. Brit. Polym. J. 1990; 22:303.
[7]   St John NA, George GA. Polymer 1992; 33:2679.
[8]   Morgan RJ, Mones ET. J. Appl. Polym. Sci. 1987; 33:999.
[9]   Lee H, Neville K., Handbook of Epoxy Resins, New York, McGraw-Hill, 1967.
[10]   Hagnauer GL, Pearce PJ. ACS Symp. Ser. 1992; 221:193.
[11]   Barton JM, Greenfield DCL. Brit. Polym. J. 1986; 18:51.
[12]   Morgan RT. Adv. Poly. Sci. 1985;72:1.
[13]   Steinmann B. J. Appl. Polym. Sci. 1989;37:1753.
[14]   Vohwinkel F. German Patent: DE 198 28 248; 1998.
[15]   Rocks J, George GA, Vohwinkel F. Polym. Int. 2003; 52:1758
[16]   Rocks J, Halter M, George G, Vohwinkel F. Polym. Int. 2003; 52:1749
[17]   Fisch W, Hofmann W. Macromol. Chem. 1961;44-46:8.
[18]   Fisch W, Hoffmann W, Kaskikallio J. J. Appl. Chem. 1956;6:429.
[19]   Fisch W, Hofmann W. J. Polym. Sci. 1954; 12:497.
[20]   O'Neill LA, Cole CP. J. Appl. Chem. 1956; 6:356.
[21]   Stevens GC. J. Appl. Polym. Sci 1981; 26:4279.
[22]   Stevens GC. J. Appl. Polym. Sci 1981; 26:4259.
[23]   Tanaka Y, Kakiuchi J. J. Appl. Polym. Sci. 1963; 7:1063.
[24]   Smith B., Infrared spectral intepetation - A systematic approach, 1 ed., New York, CRC Press LLC, 1999.
[25]   Dyke SF, Floyd AJ, Sainsbury M, Theobald RS., Organic Spectroscopy - An Introduction, London, Longman ,1978.
[26]   Pretsch E, Bühlmann P, Affolter C., Structure Determination of Organic Compounds, Berlin, Springer Publisher, 2000.
[27]   De Bakker CJ, George GA, St John NA. Spectrochim. Acta 1993;49A:739.
[28]   Walton JR, Williams KPJ. Vibr. Spectrosc. 1991;1:339.
[29]   Antoon MK, Koenig JL. J. Polym. Sci., Polym. Chem. Ed. 1981;19:549.
[30]   Agbenyega JK, Ellis G, Hendra PJ, Maddams WF, Passingham C, Willis HA, Chalmers J. Spectrochim. Acta 1990;46A:197.
[31]   Zweifel H, Völker T. Die Makromolekulare Chemie 1973;170:141.
[32]   Ricca G, Severini F. Polymer 1988;29:880.
[33]   McCormick CL, Chang Y. Macromolecules 1994;27:2151.
[34]   Simms JA, Corcoran PH. Progress in Organic Coatings 1995;26:217.
[35]   Bhadani SN, Sahu SU, Kundu S. Indian Journal of Technology 1982;20:118.
[36]   Fischer RF. Journal of Polymer Science 1960;44:155.
[37]   Luston J, Manasek Z, Kulikova M. Journal of Macromolecular Science and Chemistry 1978;A12:995.
[38]   Oh JH, Jang J, Lee SH. Polymer 2001;42:8339.
[39]   Kenny JM, Apicella A, Nicolais L. Polym. Eng. Sci. 1989;29:973.
[40]   Pascault J.P., Sautereau H., Verdu J., Williams R.J.J., Thermosetting Polymers, Marcel Dekker, New York, (2002)
[41]   Matejka L., Pokorny S., Dusek K., Macromol. Chem. 1985; 186:2025.

[42] Mauri A.N., Galego N., Riccardi C.C., Williams R.J.J., Macromolecules 1997*;* 30:1616

[43] Leukel J., Burchard W., Krüger R.P., Munch H., Schulz G., Macromol. Rapid Commun. 1996; 17:359.

[44] Fedtke M., Domaratius F., Polymer Bull. (Berlin), 1986; 15:13.

[45] Riccardi C.C., Dupuy J., Williams R.J.J., J. Polym. Sci. Part B*,* 1999, 37:2799 (1999)

[46] Galante M.J, Oyanguren P.A., Andromaque K., Frontini P.M., Williams, R.J.J., Polym. Int. 1999; 48:642

Figures and Tables

N,N,N',N'-Tetraglycidyl-4,4'-

diaminodiphenylmethane (TGDDM)

(Araldite®MY721)
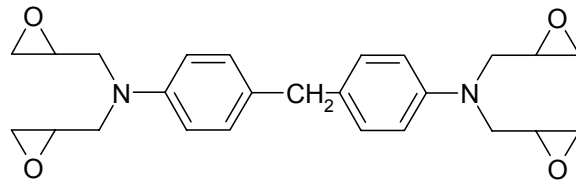
Maleic anhydride (MA)
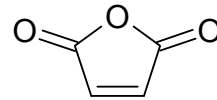
Hexahydrophthalic anhydride (HHPA)
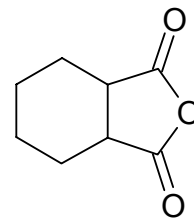
Fig. 1. Chemical structures of the materials used

a)

k_1 (1)

R1—OH

COO—R1
COOH

R1—OH + ... → COO—R1 / COOH

k_2 (2)

COO—R1 / COOH + CH$_2$—CH—CH$_2$—R2 → COO—R1 / COOCH$_2$—CH—OH / CH$_2$—R2

(3)

COO—R1 / COOCH$_2$—CH—OH / CH$_2$—R2 + → COO—R1 / COOCH$_2$—CH—O / CH$_2$—R2 ... HO—CO ... O

Cat. (4)

CH$_2$—CH—CH$_2$—R$_1$ + HO—R$_2$ → R$_2$—O—CH$_2$—CH—CH$_2$—R$_1$ / OH

b)

(5)

R1—CH—CH$_2$ + :NR$_3$ → R1—CH—C—$^+$NR$_3$ / O$^-$ / H$_2$

(6)

R1—CH—C—$^+$NR$_3$ / O$^-$ / H$_2$ + R2 ... O ... R2 → R2—CO—O—CH(R1)—CH$_2$—$^+$NR$_3$ / R2—CO—O$^-$

(7)

R2—CO—O—CH(R1)—CH$_2$—$^+$NR$_3$ / R2—CO—O$^-$ + R1—CH—CH$_2$ / O → R2—CO—O—CH(R1)—CH$_2$—$^+$NR$_3$ / R2—CO—O—CH$_2$—CH—O$^-$ / R1

(8)
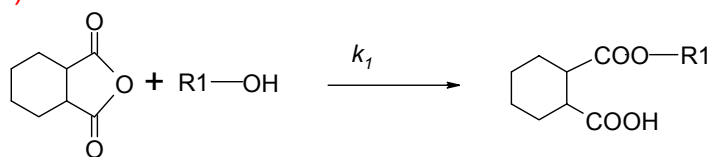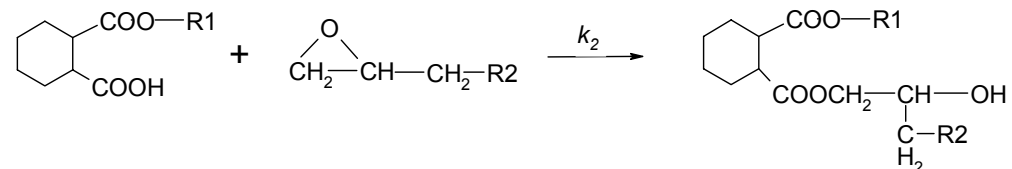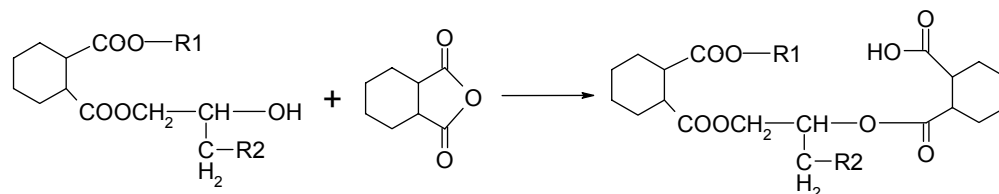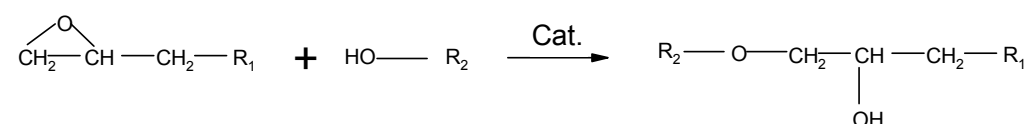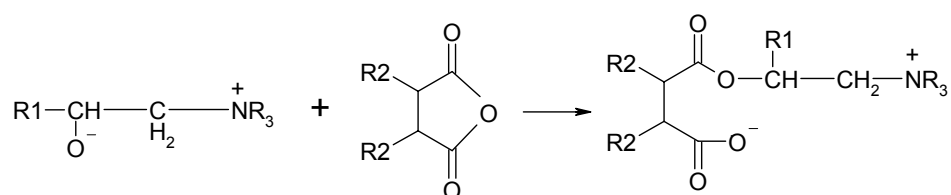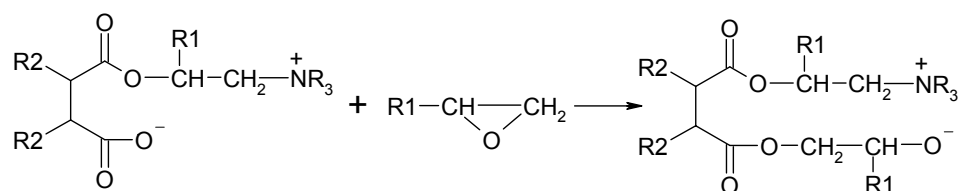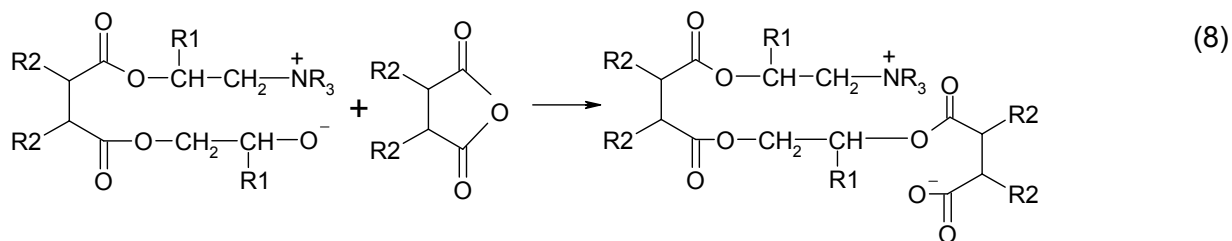
Fig. 2. Schematic cure mechanism of (a) uncatalyzed epoxy/anhydride addition reaction (reactions (1) to (3)). Reaction (4) occurs at higher temperatures and is catalyzed by anhydride or carboxyl groups.The hydroxyl group is present in the epoxy monomer.
(b) base catalyzed epoxy/anhydride reaction (reaction (5) to (8)
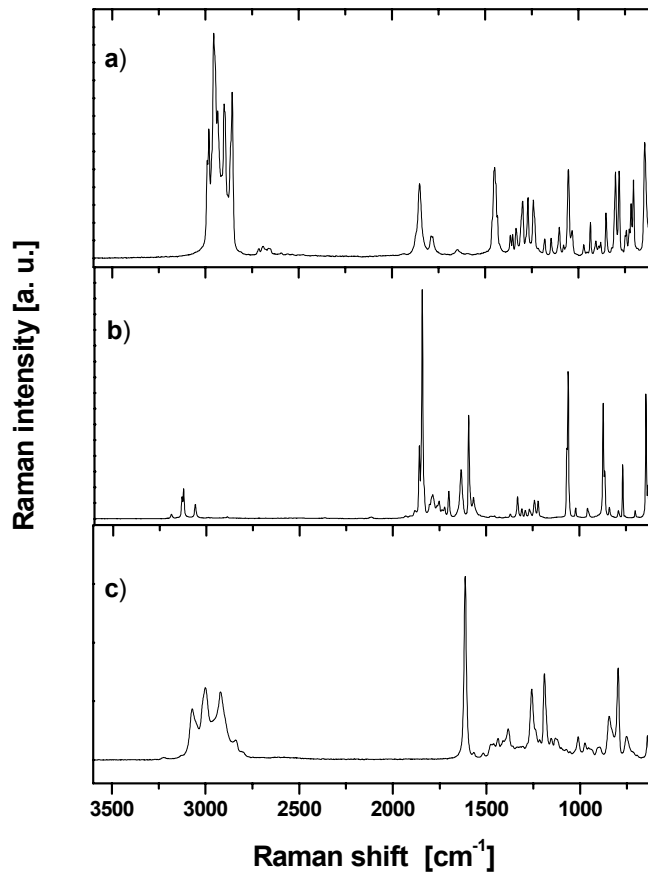
Fig. 3. FT-Raman spectra of unreacted anhydride hardeners (a) hexahydrophthalic anhydride; (b) maleic anhydride and epoxy monomer (c) Araldite[®]MY721

Table 1: Raman spectral peak assignments of (a) carboxylic acid anhydrides and (b) epoxy monomer [21-29]

a)

Peak [cm^{-1}]	Assignment
3060, 3180	ν =C-H; often multiplet
3000-2840	ν C-H aliphatic, often multiplet
1850	ν_s C=O
1780	ν_{as} C=O
1590	ν C=C (cis-configuration)
1449	δ CH$_2$
1270	δ C-H
1170-1250	ν C-O of an anhydride
1055-1060	ν_{as} C-O-C
868	νC-C-O-C-C + γ C-H in case of alkene
780	γ CH$_2$
760	δ =CH
636	γ C=C (cis-configuration)

b)

Peak [cm^{-1}]	Assignment
3072	ν_{as} C-H of epoxide.
3001	ν_s C-H of epoxide
2940-2915	ν_{as} C-H in CH$_2$
2840	ν_s C-H in CH$_2$
1614	Quadrant stretching of benzene ring
1470	δCH$_2$ (scissoring) + δ_{as} CH$_3$
1382	δ_sCH$_3$
1260	ν breathing of the epoxide ring
1190	δ aromatic C-H (in plane)
1012	δ aromatic C-H
907	ν_{as} def of the oxirane ring
846	ν_s def CH$_2$ of oxirane ring
799	mono substituted benzene
750	CH$_2$ skeletal
640	p-sub benzene ring (mono substituted benzene)
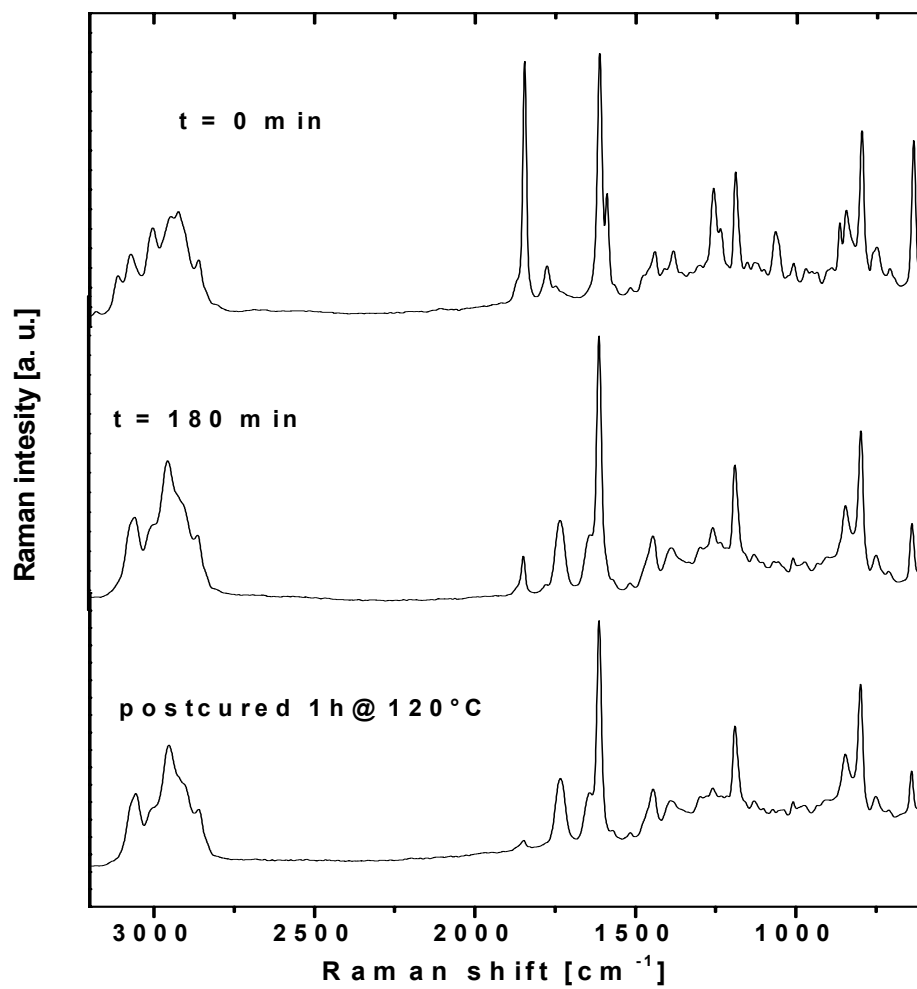
Fig. 4. FT-Raman spectra of MY721/MA/HHPA at various extents of cure at 65°C and after 1 hour postcuring at 120°C.
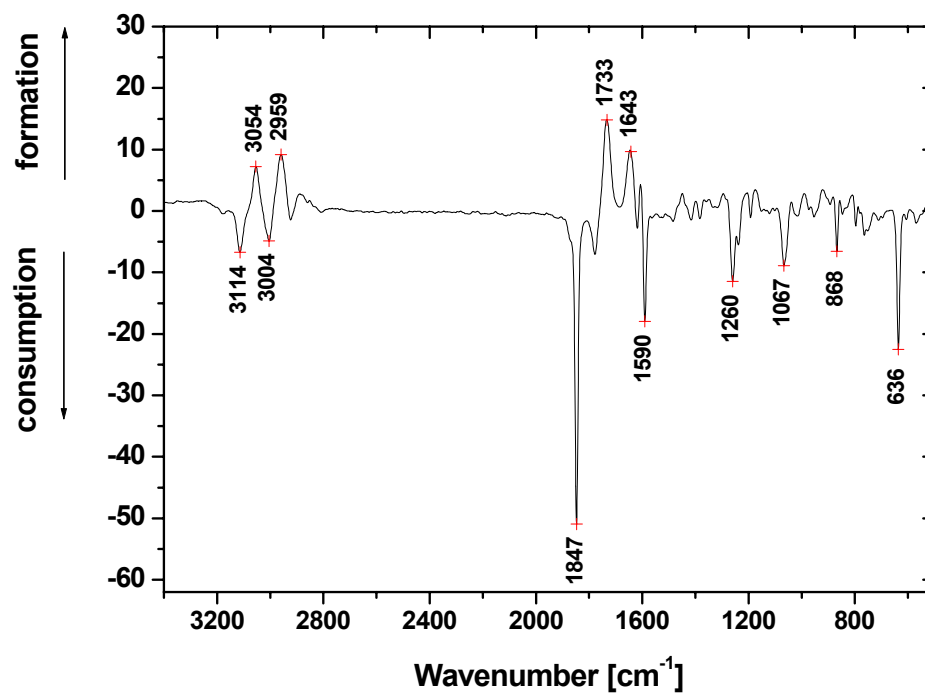
Fig. 5. Difference of FT-Raman spectra obtained by spectrum "after 1hour at 120°C" minus spectrum "uncured" directly after mixing of the MY721/MA/HHPA system. Changes in peaks marked with a symbol are discussed in the text.
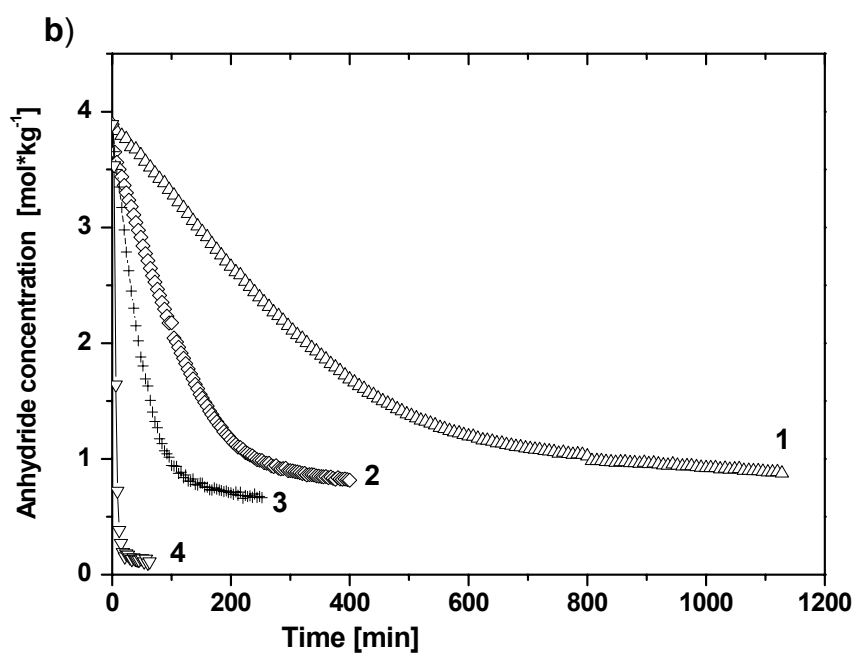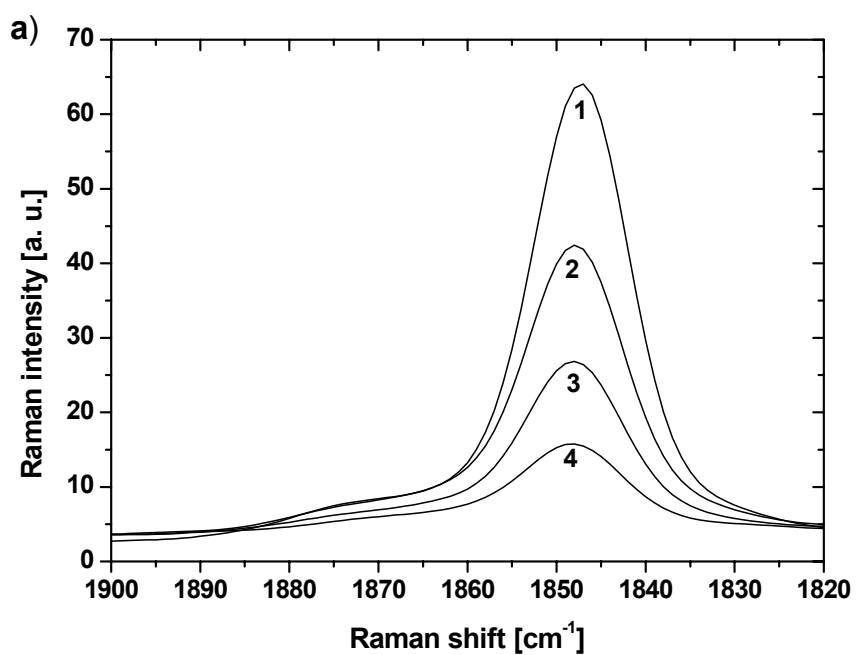
Fig. 6. (a) FT-Raman spectra of anhydride peak [1850cm^{-1}] at (1) 0, (2) 30, (3) 60, (4) 120 min of cure at 75°C. (b) Plot of anhydride group concentration versus cure time at (1) 55°C, (2) 65°C, (3) 75°C, (4) 100°C
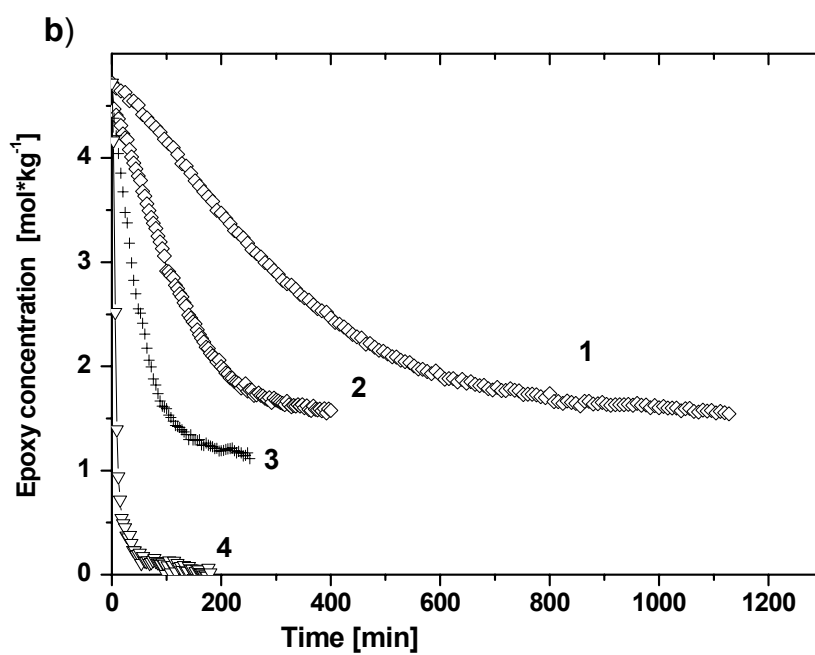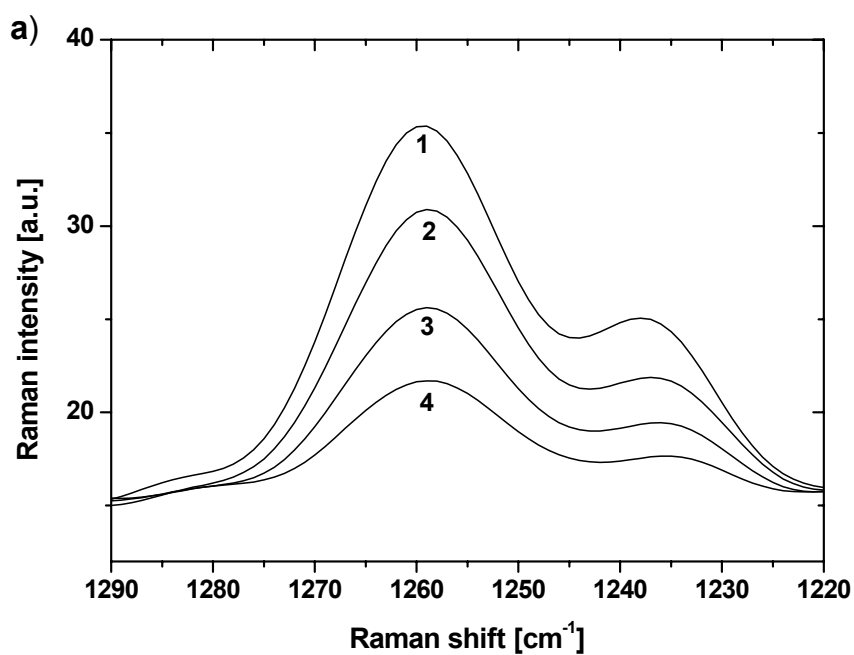
Fig. 7. (a) FT-Raman spectra of epoxy peak [1260cm^{-1}] at (1) 0, (2) 30, (3) 60, (4) 120 min of cure at 75°C. (b) Plot of epoxy group concentration versus cure time at (1) 55°C, (2) 65°C, (3) 75°C, (4) 100°C.
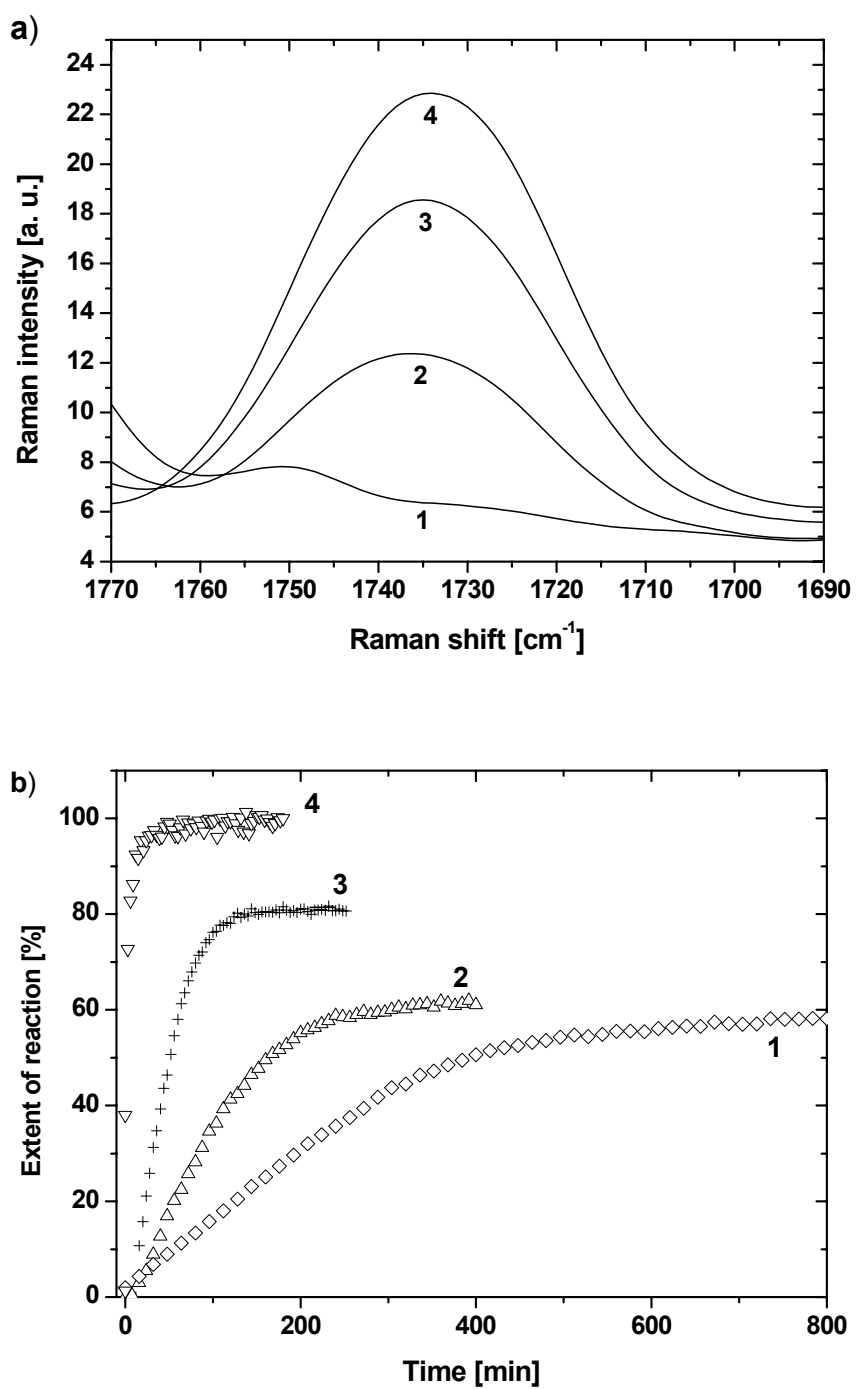
Fig. 8. (a) FT-Raman spectra of aliphatic ester peak [1734 cm^{-1}] at (1) 0, (2) 30, (3) 60, (4) 120 min of cure at 75°C; (b) plot of extent of ester group reaction versus cure time at (1) 55°C, (2) 65°C, (3) 75°C, (4) 100°C
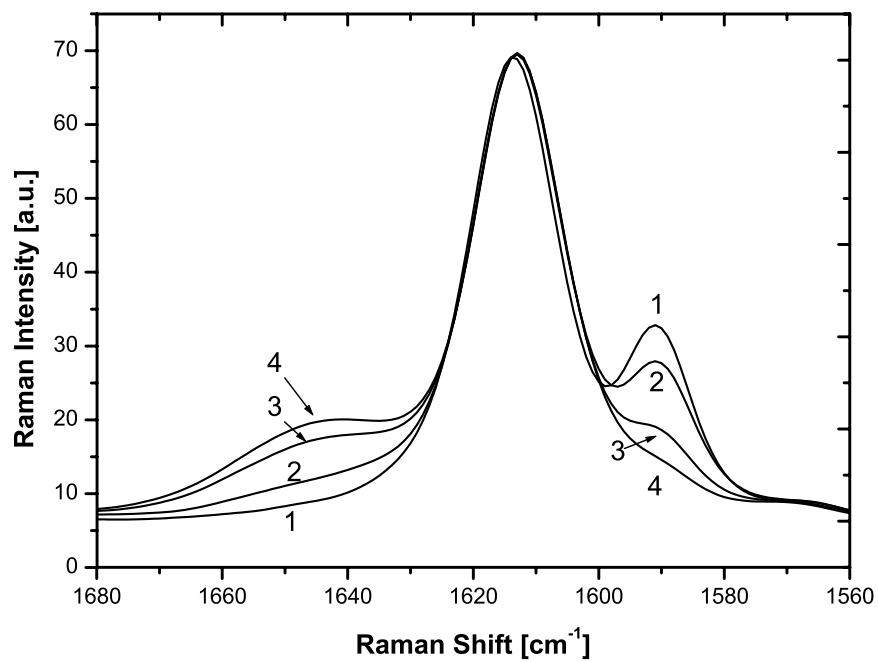
Fig. 9(a) FT-Raman spectra at (1) 0, (2) 30, (3) 60, (4) 120 min of cure at 75°C.
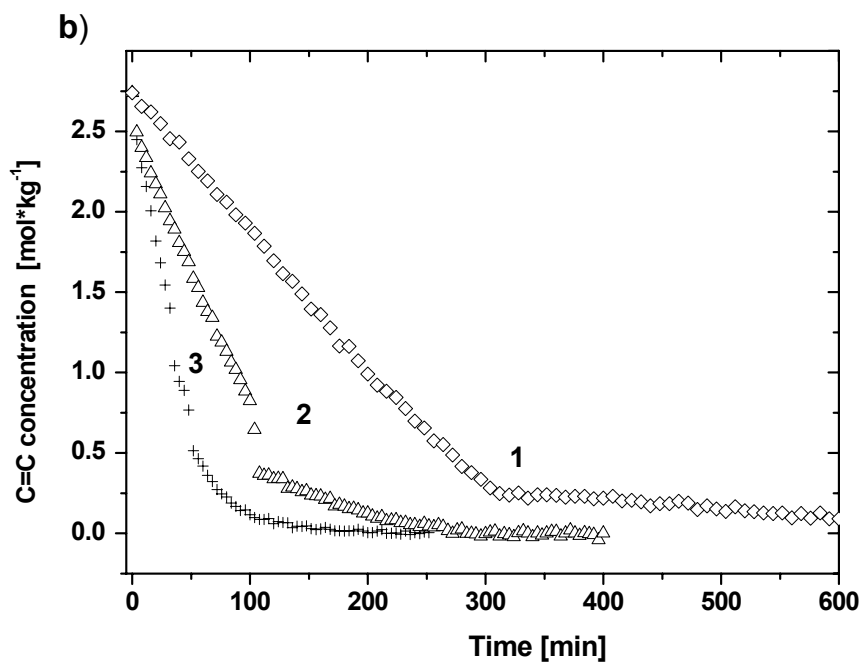
Fig. 9.(b) Plot of change in band intensity at 1590 cm^{-1} expressed as [C=C] in MA.

c)
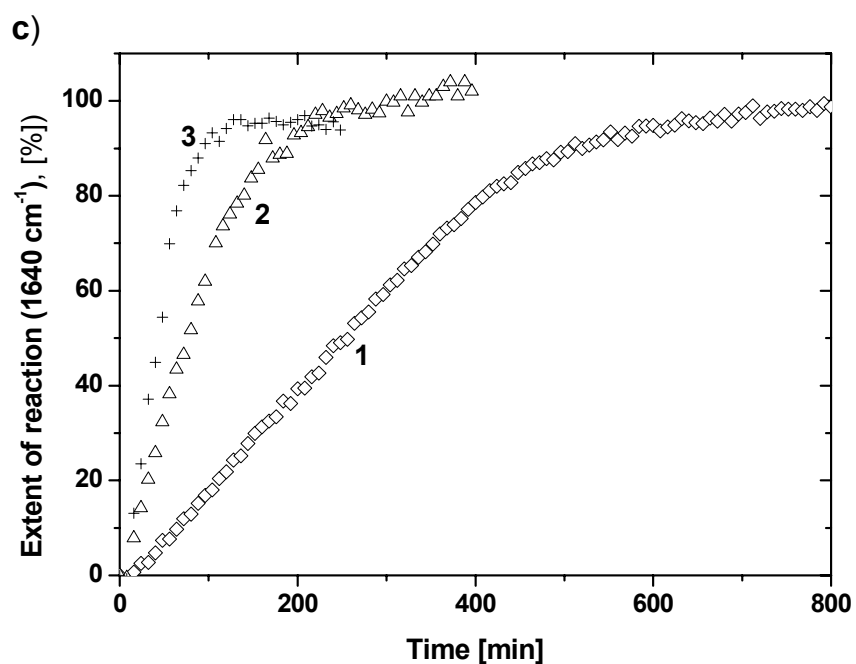
Fig. 9. (c) Newly formed 1640 cm^{-1} peak intensity versus cure time as a function of isothermal curing temperature: (1) 55°C, (2) 65°C, (3) 75°C

(1)

(2)

(3)
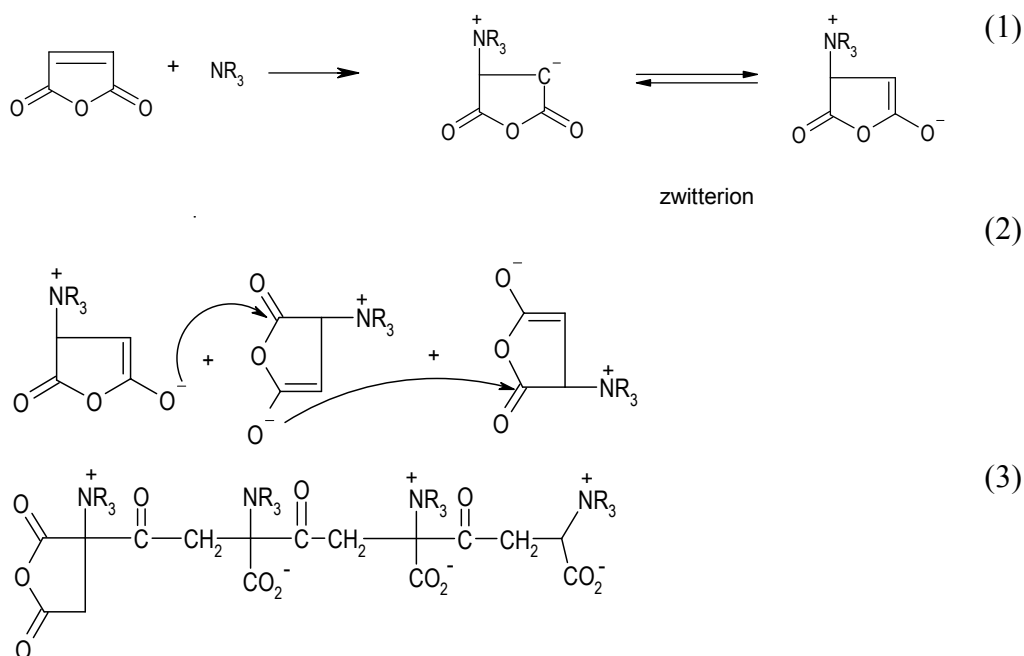
Fig. 10. Proposed reaction mechanisms of maleic anhydride in the presence of tertiary amine according to Zweifel et al. [31]
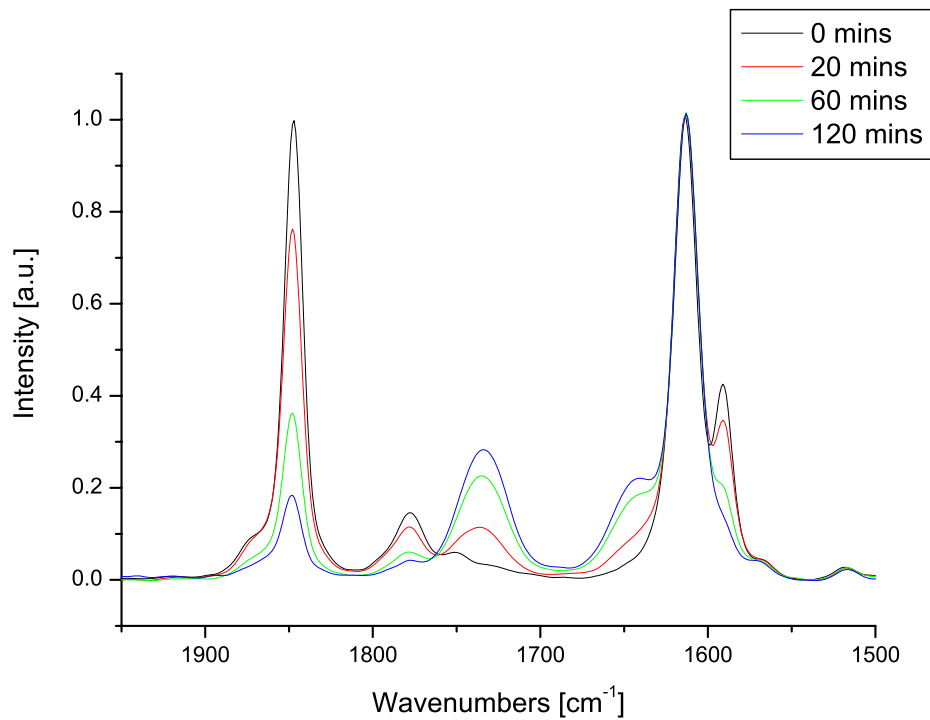
Fig 11(a) Expanded region of FT-Raman spectrum during the cure of TGDDM with MA/HHPA at 75°C showing isosbestic point at 1760 cm^{-1}.
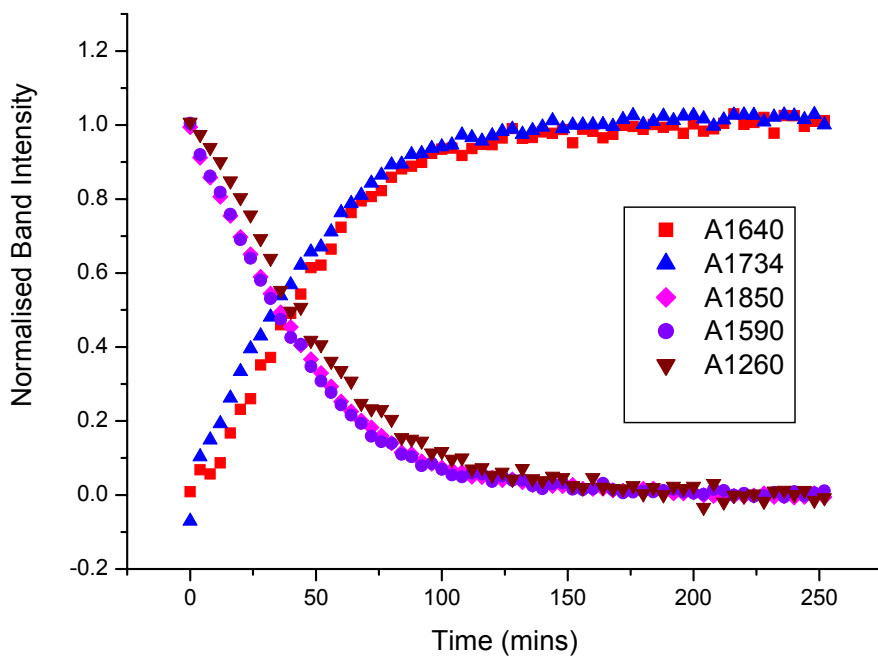
Fig 11(b) Plot of band areas from Fig 11(a) indicating the similarity in the rates of disappearance of the bands at 1850, 1590 and 1260 cm^{-1} and the rate of appearance of the bands at 1640 and 1730 cm^{-1}.
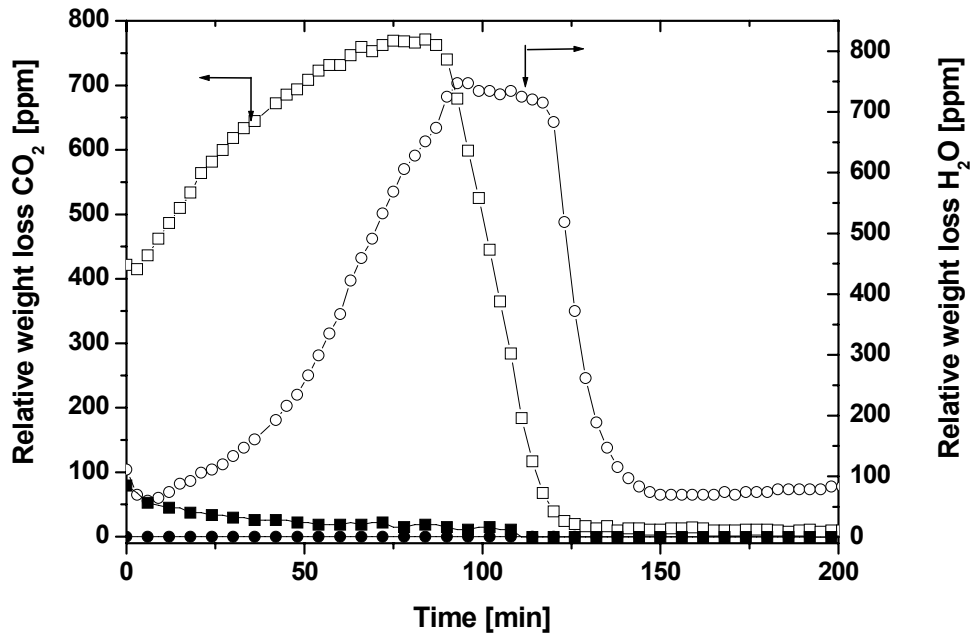
Fig. 12: Released carbon dioxide (■, □) and water (●, ○) as determined by *in situ* gas chromatography (GC) during isothermal cure at 65°C. Open symbols reflect the MY721/MA/HHPA-system and closed symbols denote the MY721/HHPA-system

Table 2: First order rate constants and time of deviation as function of curing temperature for the investigated MY721/MA/HHPA-system as measured by FT-Raman.

Temperature	Anhydride (k^*_1)	Epoxide (k^*_2)	$t_{deviation}$ [sec]
55°C	3.5e-5	2.9e-5	27360
65°C	5.7e-5	4.5e-5	15120
75°C	26.1e-5	19e-5	5880
100°C	3.5e-3	2.7e-3	1260

a)

b)

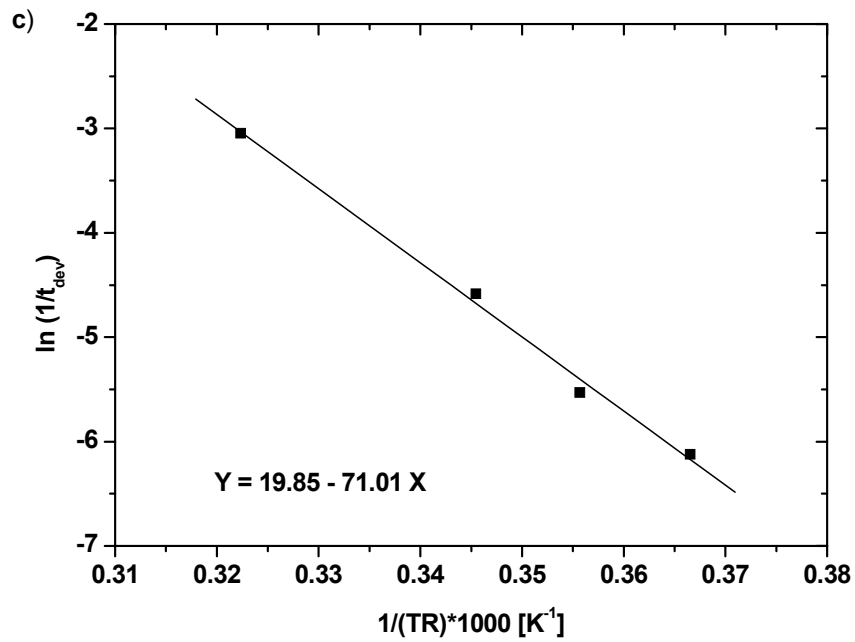71%

70%

67%

c)

$Y = 19.85 - 71.01 \ X$
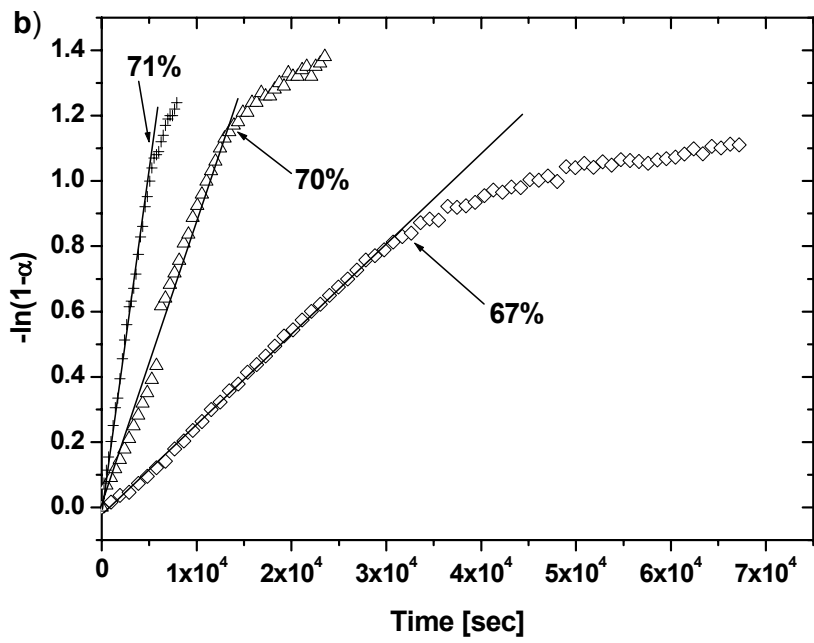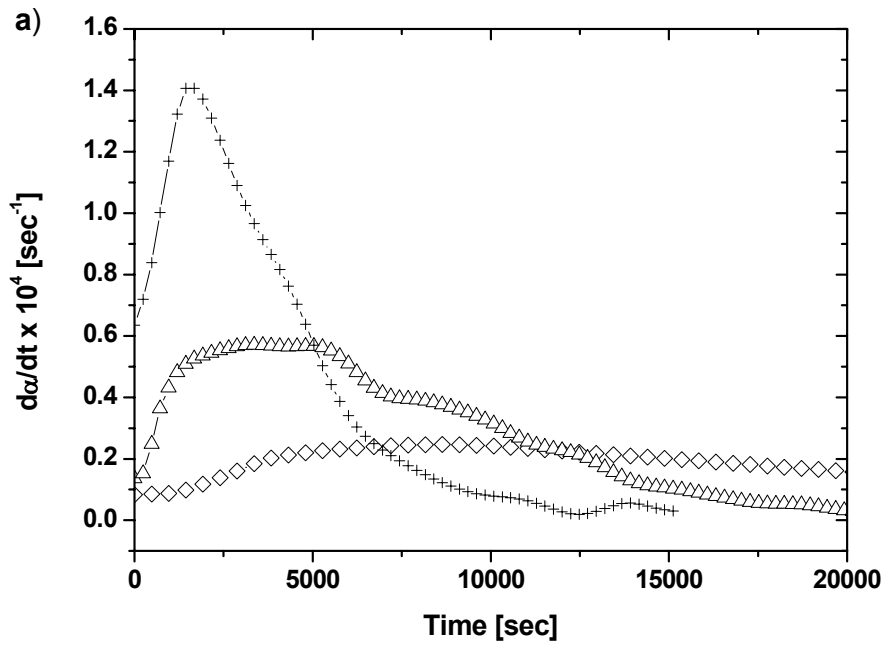
Fig.13. (a) Plot of the empirical epoxide reaction rate $-d[EP]/dt$ as function of curing time;(b) first order kinetic regression plot of epoxide reaction, for 55°C (M), 65°C(8), 75°C (+) as measured by FT-Raman; (c) Arrhenius plot of the time to deviation
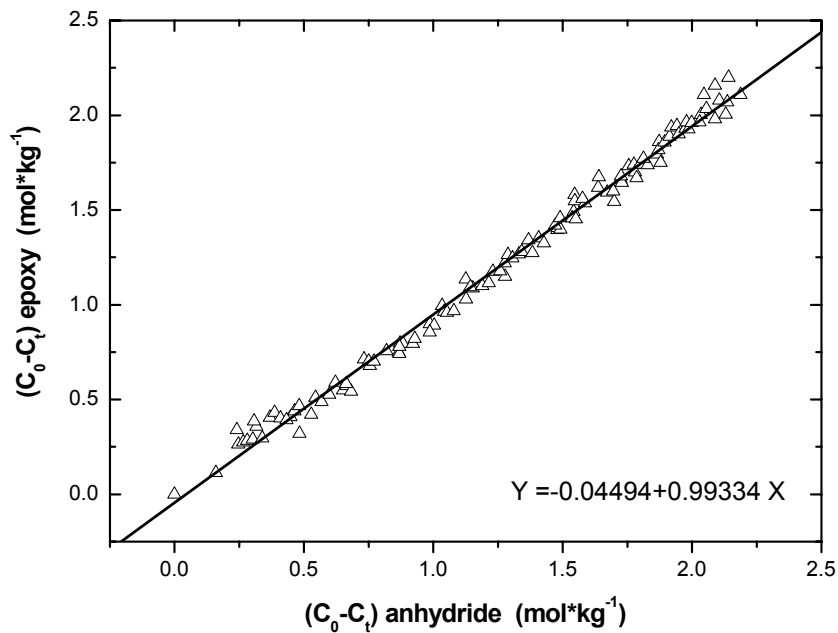

$Y = -0.04494 + 0.99334 \ X$

Fig. 14. Absolute conversion of epoxy groups versus absolute conversion of anhydride groups obtained from FT-Raman experiments at 65°C. Molar anhydride to epoxy ratio, r=0.8